

THE YF-12 GUST VELOCITY MEASURING SYSTEM

L. J. Ehernberger
Dryden Flight Research Center

SUMMARY

A true gust velocity measuring system designed to alleviate complications resulting from airframe flexibility and from the high-speed, high-temperature environment of supersonic cruise aircraft was evaluated on a YF-12 airplane. A unique feature of the system is the use of fixed vanes on which airflow direction changes produce differential pressure variations that are measured. Airframe motions, obtained by postflight integration of recorded angular rate and linear acceleration data, are removed from the flow angle data.

An example of turbulence data obtained at high-altitude, supersonic flight conditions is presented. Comparisons are made with previous high-altitude turbulence measurements obtained with subsonic aircraft and with turbulence criteria contained in both military and civil design specifications for supersonic cruise vehicles. Results of these comparisons indicate that the YF-12 turbulence sample is representative of turbulence present in the supersonic cruise environment.

INTRODUCTION

Turbulence characteristics in the supersonic cruise environment have been measured by subsonic aircraft up to an altitude of 22 kilometers. References 1 to 3 present subsonic aircraft data for true gust velocity measurements and for derived equivalent gust velocities based on airplane gust acceleration loads. These data have been verified to a limited extent by supersonic measurements reported in references 4 to 6. However, as supersonic airframe and system designs become more refined, the need arises to obtain true gust velocity measurements to evaluate the effects of turbulence on aircraft and flight systems designed to operate in the supersonic flight environment (ref. 7).

A variety of instrument configurations has proven practical for gust measurements on subsonic aircraft. However, the gust velocity errors due to flow angle measurement errors increase in direct proportion to speed. Therefore, the angular resolution requirements for supersonic cruise measurements are increasingly more stringent as the flight speed increases. Additional complications are also encountered in the separation of sensor motions due to aircraft maneuvering from the gust flow

direction measurements. This is due to the combined effects of structural flexibility and the higher flight speeds.

In general, the magnitude of airframe bending is greater at the lower frequencies. At high speeds, the structural frequencies are superimposed on longer gust wavelengths having greater turbulent energy. This contrasts with conditions encountered in subsonic flight, where significant bending is usually limited to the shorter gust wavelengths with less turbulent energy and with highly repeatable spectral patterns. Thus, at supersonic cruise conditions, the measurement of airflow motion at the structural bending frequencies requires the use of sensors having greatly improved amplitude resolution and phase matching capabilities. An additional complication results from aerodynamic heating which can deteriorate the performance of movable, low-inertia flow direction vanes at the higher Mach numbers (ref. 6). The presence of heating also requires special consideration in the selection and installation of transducers.

A true gust velocity measurement concept designed to alleviate these complications is being evaluated in the supersonic cruise environment using the YF-12 airplane. This report describes the system used to obtain measurements of longitudinal, vertical, and lateral components of gust velocity. It also presents a preliminary example of turbulence data obtained during supersonic cruise at approximately 19.8 kilometers altitude. These data are compared with measurements obtained with subsonic aircraft and with turbulence criteria contained in current civil and military design specifications applicable to supersonic cruise vehicles.

SYMBOLS

Physical quantities in this report are given in the International System of Units (SI).

a_x	lateral acceleration
a_y	longitudinal acceleration
a_n	vertical acceleration
C_{p_α}	pressure coefficient for gust vane angle of attack
C_{p_β}	pressure coefficient for gust vane angle of sideslip
l_x	linear longitudinal distance from gust vane to reference instruments
l_y	linear lateral distance from gust vane to reference instruments
l_z	linear vertical distance from gust vane to reference instruments
M	free stream Mach number
p	roll attitude angular rate

p_{dl}	differential pressure between the dog-leg total pressure source and p_{t_2}
p_{t_2}	measured nose boom total pressure
p_α	differential pressure between lower and upper ports of the angle-of-attack vane
q	pitch attitude angular rate
q_∞	incompressible dynamic pressure
R_t	ratio of dog-leg total pressure to p_{t_2}
r	yaw attitude angular rate
u	longitudinal gust velocity
V	true airspeed
v	lateral gust velocity
w	vertical gust velocity
\dot{z}	airplane vertical velocity (positive down)
α	free stream angle of attack
β	free stream angle of sideslip
Δ	incremental change
θ	pitch attitude
ϕ	roll attitude

INSTRUMENTATION

The primary components of the true gust velocity system are the sensors used to measure airflow angle changes and true airspeed variations. Differential pressures across four fixed-flow direction vanes near the base of the nose boom are used to determine airflow direction. The vanes are arranged in a cruciform configuration, as shown in figure 1. Two of the vanes independently measure angle of sideslip, while the remaining two vanes independently measure angle of attack. This configuration provides measurement redundancy and minimizes asymmetric aerodynamic interference between the vanes.

The vanes are constructed of stainless steel in a triangular planform. They have a leading edge sweep angle of 66.5° and a thickness of 3.18 centimeters. Each vane is tapered with a 30° semiwedge angle (fig. 1(c)) to prevent oblique shock attachment. This enhances its pressure sensitivity to flow angle changes at high Mach numbers.

Figure 1(c) shows the slotted pressure sources on either side of each vane. The differential pressures across each of the vanes are measured by transducers located in the nose section of the aircraft. Insulation and air conditioning are used to maintain instrument temperatures below 313 K. The sensitivity of the vane differential pressure is also increased by the wing-body effect of the vanes attached to the boom. Positioning the vanes near the base of the boom avoids interference with the airplane's flow direction sensor and static sources located on the forward portion of the boom. It also minimizes the length of tubing and resulting pressure lag so that phase and amplitude errors are negligible below about 20 hertz.

In addition to gust inputs, the measured flow direction is also a function of the motion of the fixed vane and its nose boom mounting. Translational and rotational inputs are sensed with three-axis linear accelerometers and angular rate gyros aligned to the nose boom axis and mounted adjacent to the vane pressure sensors.

Although normally it would have been desirable to use the nose boom pressure source to determine longitudinal gust velocities, the length of the YF-12 nose boom would have caused excessive tubing lag. It was not possible to install a transducer in the forward portion of the boom since all available space was already occupied by tubing used for the primary airplane instruments. However, even if space had been available, the elevated temperatures present in the boom during high-speed flight made the location unsuited for transducer use. Therefore, the longitudinal gust velocity was sensed by means of a dog-leg pitot probe that was attached to the lower surface of the nose, approximately 3.5 meters aft of the nose boom (fig. 2). A differential pressure transducer using the nose boom total pressure as a reference measured the local pitot pressure at the probe. Using the dog-leg pitot probe, the length of the pitot lines was kept to less than one meter. This provided good frequency response up to approximately 20 hertz and permitted the transducer to be installed in the air conditioned instrument compartment in the nose of the aircraft.

To avoid phase errors and minimize mechanically induced signal errors, sensor dynamic characteristics were carefully scrutinized in the selection process. Resolution and phase errors were also minimized using a special 13-bit analog-to-digital encoder. Signals digitized by the encoder were synchronously read and recorded in each PCM time frame. The data acquisition system acquired each parameter measurement at the rate of 200 samples per second. Parameter characteristics are provided in table 1.

Auxiliary data parameters used in the gust calculations included airplane Mach number, airspeed, altitude, free stream ambient temperature, roll attitude, and pitch attitude. The instruments and systems used to measure these parameters are described in references 8 and 9.

DATA ANALYSIS PROCEDURES

Lateral and Vertical Gust Velocities

The true gust velocity calculations were based primarily on the angle-of-attack and angle-of-sideslip changes caused by the turbulence. The measured flow angles were corrected for aircraft motion and then the gust time history was calculated by multiplying the sine of the incremental flow angle by the true airspeed. To accomplish this, the gust vane pressure data were first normalized to coefficient form and converted to flow angle information. The gust vane flow angle pressure coefficients were obtained using the incompressible dynamic pressure, q_∞ , as shown in the following equation:

$$C_{p_\alpha} = \frac{p_\alpha}{q_\infty} \quad (1)$$

where C_{p_α} is the gust angle-of-attack pressure coefficient and p_α is the differential pressure between the lower and upper sources of the angle-of-attack vane. Calibration of the gust vane pressure coefficients in terms of airplane free stream flow direction was accomplished by fitting data obtained for in-flight maneuvers at several Mach numbers using fifth order polynomials. The polynomial curves resulting from the calibration maneuvers for the Mach number range from 2.2 to 2.8 are shown in figure 3(a).

To calculate the lateral and vertical gust velocities, the flow angle changes and rates were corrected for angular attitude changes and rates as shown by the equation for the vertical gust component, w .

$$w = V \sin \left[\left(\Delta\alpha + \frac{q}{V} l_x - \frac{p}{V} l_y \right) \cos \varphi + \left(\Delta\beta - \frac{r}{V} l_x - \frac{p}{V} l_z \right) \sin \varphi - \Delta\theta \right] - \Delta\dot{z} \quad (2)$$

The angular rate effect on the flow angles was removed by using the measured roll, pitch, and yaw attitude rates, p , q , and r , respectively. The true airspeed, V , and the linear distances from the reference instruments, l_x , l_y , and l_z , measured along the longitudinal, lateral, and vertical axes were used in the form $\frac{q}{V} l_x$, as shown in equation (2). Next, the incremental flow angles, $\Delta\alpha$ and $\Delta\beta$, were resolved into components along the earth reference axes using the sine and cosine functions of the nose roll attitude, φ . To complete the vertical gust velocity calculation, the incremental pitch attitude changes, $\Delta\theta$, were subtracted from the incremental earth referenced angle of attack. The sine of the resulting angle was multiplied by the true airspeed, and the incremental vertical translation velocity, $\Delta\dot{z}$, was subtracted from the resulting term.

The nose roll attitude, φ , used in the gust velocity equation, was obtained by transforming the airplane inertial platform attitude data from airframe reference coordinates to the nose boom axes. Frequency-response and phase shift problems associated with direct attitude measurements were circumvented by integrating

angular rate data from a special high response, low drift gyro to obtain the incremental pitch and yaw attitude changes of the gust vanes. The rate data were first transformed to earth reference coordinates and then integrated. Incremental vertical and lateral translation velocity changes were determined in a similar manner. The linear acceleration measurements were corrected for the earth's gravitational component and transformed to earth referenced coordinates using the inertial platform attitude data. Then, after the mean values of each component were determined and removed to minimize drift, the data were integrated to obtain the velocity changes.

Longitudinal Gust Velocity

The longitudinal component of gust velocity was obtained by using the ratio of the local total pressure at the dog leg to the nose boom total pressure. In equation form this is given by

$$R_t = \frac{p_{dl} + p_{t_2}}{p_{t_2}} \quad (3)$$

where the differential pressure measured between the dog leg and the nose boom is designated as p_{dl} and the nose boom total pressure is designated p_{t_2} . At supersonic

Mach numbers, R_t becomes sensitive to angle of attack, so a correction was applied.

The correction increased linearly with C_{p_α} and with the parameter $\sqrt{M^2 - 1}$, where

M is the free stream Mach number. A Mach number which includes the gust input was obtained from the corrected R_t by means of a fifth order polynomial determined from flight data for Mach number acceleration and deceleration runs. The polynomial curve for the Mach numbers from 2.0 to 2.8 is shown in figure 3(b). This Mach number, which is responsive to gusts, was then multiplied by the speed of sound to give the true velocity units. The longitudinal gust velocity time history was then computed using first order regression analysis to remove the mean value and the trend from the true airspeed time history.

In contrast to the airplane reference used for longitudinal velocity, the lateral and vertical velocity components were resolved into earth referenced components as described. Differences due to the referencing convention were negligible for the gust data presented because airplane attitude and ground speed changes were minimal. However, the differences would be significant in the case of maneuvering flight.

Statistical Analyses

Spectral and statistical analyses of the data were used to eliminate errors caused by electrical transients in the instrumentation or by bit errors accumulated during the recording and processing of the digital data. This was accomplished by screening parameters of interest for sample-to-sample changes that were larger than values which were specified to discriminate between physically realistic measurement changes and extraneous data points. When found, such values were replaced with

the last valid data value. While this procedure did not restore the true values to the time history data, it did eliminate significant spectral and statistical distortion from most data records.

The spectral and statistical analyses were accomplished by a library program which uses a fast Fourier transform. The analysis routine included detrending the parameters and filtering with a fourth order Butterworth filter having a 3-decibel break point at 16 hertz. As with the spike removal, the detrending and filtering eliminated unwanted spectral content that would have otherwise concealed gust or transient spectral phenomena of interest.

RESULTS AND DISCUSSION

To illustrate the type of turbulence data encountered on the YF-12 flights, one of the stronger turbulence encounters was selected. This encounter, rated as having a light-to-moderate intensity by the aircrew, occurred during a deceleration from Mach 2.75 to Mach 2.69, between altitudes of 19.8 and 19.9 kilometers. A steady wings level condition was held throughout the encounter and the pitch attitude change was less than 0.3° . The longitudinal, lateral, and vertical gust velocity time histories were obtained using calculations previously described and are shown in figure 4. Their intensity appears to be stationary in a statistical sense; however, at the lower frequencies or longer wavelengths, the longitudinal component exhibits noticeably stronger quasi-periodic variations than do the lateral and vertical components.

Probability density plots for these data may be compared to normal probability density functions having the same mean and variance values, as shown in figure 5. It was assumed that the deviations from the plots of the normal curves were due to the relatively short record length.

The power spectra shown in figure 6 were obtained using eight degrees of freedom and a seven-point Hann-Tukey smoothing window. The relatively higher spectral density amplitudes of the longitudinal component at long wavelengths are indicative of the quasi-periodic long period characteristics noted in the time histories. The differences in the spectral densities of the component gust velocities at the longer wavelengths also significantly influence the comparison of the component root-mean-squared (rms) velocities. The rms velocity for the total spectral range was 2.15 meters per second for the longitudinal component in contrast to rms gust velocities of about 1.21 and 1.16 meters per second for the lateral and vertical components. However, for the spectral range limited to wavelengths less than 667 meters, which was selected for comparison with other data, the rms velocities for the three components were close, with 0.82 meter per second for the longitudinal component compared to 0.67 and 0.83 meters per second for the lateral and vertical components. Thus, both the rms gust velocities and the spectral density properties are important measures of the turbulence intensity.

Inaccuracies in the gust data may be attributed to three sources: system noise errors, dynamic matching and response errors, and calibration inaccuracies. Although a thorough analysis of the errors present in the preliminary data sample has not yet been completed, preliminary studies of the data for several turbulence

encounters indicate that the rms noise level is probably on the order of 0.2 meter per second or less. Over the measurement ranges used, calibration precision of the fast response Mach number and flow direction sensors is high relative to the basic airplane Mach number and flow angle measurements. However, the gust sensor calibrations are nonlinear and gust measurement accuracy can be affected by slope changes occurring within small measurement ranges. In addition, instrument drift may not be linear with time and thus may not be completely eliminated by subtracting the mean values or by detrending. The combination of calibration and drift errors are estimated to cause about 10-percent error in the measured gust velocities. Resultant rms gust velocity errors in the preliminary data appear to be on the order of 0.3 to 0.4 meter per second.

The intensity of the preliminary YF-12 turbulence data was compared to previous data obtained using subsonic aircraft and to intensity factors contained in established design criteria. Presented in figure 7 are the widely depicted examples of clear air turbulence, cumulus turbulence, and thunderstorm turbulence (ref. 10). For comparison, the spectral density amplitudes for the vertical, lateral, and longitudinal time histories for the YF-12 data are indicated by shaded regions on the figure, which can be seen to lie close to the amplitude of the clear air turbulence (ref. 10) based on lower altitude measurements.

Reference 11 contains the probability distributions for the rms gust velocities for wavelengths less than 667 meters obtained from the HICAT (high altitude clean air turbulence) project using the U-2 airplane at altitudes between 14 and 22 kilometers. Data from the U-2 measurements indicated a 1.0-percent probability for rms gust velocities of 0.65, 0.69, and 0.59 meters per second or greater (longitudinal, lateral, and vertical). The same data indicated a 0.1-percent probability for rms gust velocities of 1.12, 1.15, and 0.96 meters per second or greater in the same axes. For the YF-12 turbulence sample, the measured longitudinal, lateral, and vertical rms gust velocities were 0.82, 0.67, and 0.83 meters per second. This comparison is shown in tabular form below:

HICAT probability, percent	Rms gust velocity, m/sec (wavelengths < 667 m)		
	u	v	w
1.0	0.65	0.69	0.59
0.1	1.12	1.15	0.96
YF-12 data	0.82	0.67	0.83

During the HICAT project less turbulence was experienced at altitudes near 20 kilometers than at altitudes below 19 kilometers; therefore, the rms gust velocities from the HICAT data are probably greater than they would have been had they been obtained only at the altitude of the YF-12 sample. Thus, based on the reference 11 data, the probability of encountering turbulence equal to or greater than the intensity of the YF-12 sample at 19.8 kilometers altitude is estimated at about 0.1 percent or less.

A similar comparison may be made between the intensity of the high-altitude turbulence sample and current turbulence design criteria for civil and military aircraft. For nonstorm turbulence at altitudes corresponding to that of the YF-12 sample, reference 12 specifies that turbulence having an rms gust velocity of 1.05 meters per second will be present 0.09 percent of the time. This is close to the estimated 0.1-percent probability values for measured YF-12 intensities having an rms vertical gust velocity over the total spectral range of 1.16 meters per second.

The military specification (ref. 13) establishing intensity design criteria for the YF-12 flight level is essentially the same as the civil specification. However, reference 13 also specifies discrete gust magnitudes as a function of normalized discrete gust length for the simulation of gusts or ramps having a "one-minus-cosine" shape. The magnitudes specified increase with wavelength to a maximum peak-to-peak value of 5.2 times the rms gust velocity. A comparison of the specification values with maximum peak-to-peak values contained in the YF-12 time histories (fig. 4) is shown below:

Gust velocity component	Rms gust velocity, m/sec	YF-12 peak-to-peak value, m/sec	5.2 criteria peak-to-peak value, m/sec
Longitudinal	2.15	7.0	11.2
Lateral	1.21	5.8	6.3
Vertical	1.16	4.9 to 9.7	6.0

The observed maximum amplitudes generally fall within the reference 13 criteria, as would be expected for the nominally short time histories. The higher value for the YF-12 vertical component had large velocity excursions in both the positive and negative directions, as shown at 9.3 seconds in figure 4. This is characteristic of a vortex core associated with a breaking wave and, in such cases, where turbulence is originating, neither the reference 13 criteria nor any other ensemble process statistics could be expected to apply precisely for homogeneous turbulence.

On the basis of the comparisons between the gust velocities of the YF-12 turbulence sample and those of references 11 to 13, it can be concluded that the intensity of the YF-12 sample is strong and, therefore, can appropriately represent high-altitude turbulence for supersonic cruise aircraft system response studies.

CONCLUDING REMARKS

A preliminary sample of gust data obtained using the YF-12 airplane has demonstrated the feasibility of using fixed, differential pressure flow vanes for turbulence measurements in the high-speed flight environment. The turbulence measurement system design considered the dynamic response of the instruments necessary to accurately sense the reference motion of the instrument platform as well as to accurately sense the free stream turbulence inputs. Spectra of the preliminary turbulence time histories indicate that system characteristics are adequate over a frequency range from less than 1 hertz to greater than 10 hertz, a

range which covers most of the turbulence inputs and aircraft system responses of interest. Comparisons with current design criteria and previously obtained data indicate that the intensity of turbulence measured by the YF-12 airplane is representative of strong high-altitude turbulence and is appropriate for use in system response studies for the supersonic cruise environment.

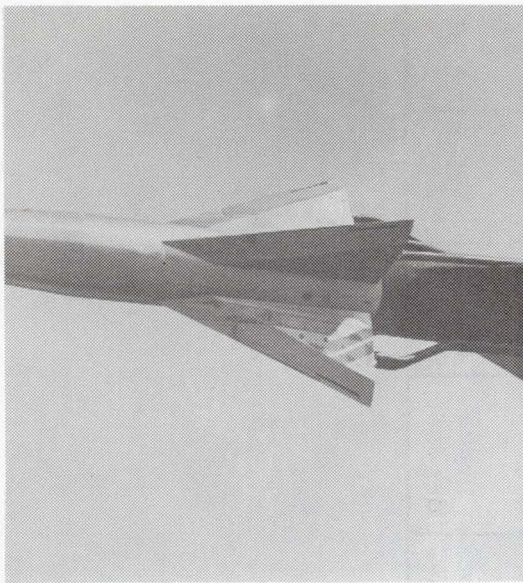
REFERENCES

1. Press, Harry; and Steiner, Roy: An Approach to the Problem of Estimating Severe and Repeated Gust Loads for Missile Operations. NACA TN 4332, 1958.
2. Coleman, Thomas L.; and Steiner, Roy: Atmospheric Turbulence Measurements Obtained From Airplane Operations at Altitudes Between 20,000 and 75,000 Feet for Several Areas in the Northern Hemisphere. NASA TN D-548, 1960.
3. Waco, David E.; and Ashburn, Edward V.: Turbulence Variations During the High Altitude Clear Air Turbulence (HICAT) Program. J. Aircraft, vol. 10, no. 1, Jan. 1973, pp. 56-58.
4. Kordes, Eldon E.; and Love, Betty J.: Preliminary Evaluation of XB-70 Airplane Encounters With High-Altitude Turbulence. NASA TN D-4209, 1967.
5. Ehernberger, L. J.; and Love, Betty J.: High Altitude Gust Acceleration Environment as Experienced by a Supersonic Airplane. NASA TN D-7868, 1975.
6. Wilson, Ronald J.; Love, Betty J.; and Larson, Richard R.: Evaluation of Effects of High-Altitude Turbulence Encounters on the XB-70 Airplane. NASA TN D-6457, 1971.
7. Boeing Commercial Airplane Company: Supersonic Cruise Research Airplane Study. NASA CR-145212, 1977.
8. Larson, Terry J.; and Ehernberger, L. J.: Techniques Used for Determination of Static Source Position Error of a High Altitude Supersonic Airplane. NASA TM X-3152, 1975.
9. Burcham, Frank W.; Montoya, Earl J.; and Lutschg, Phillip J.: Description of the YF-12 Airplane, Propulsion System, and Instrumentation for Propulsion Research Flight Tests. NASA TM X-3009, 1974.
10. Rhyne, Richard H.; and Steiner, Roy: Power Spectral Measurement of Atmospheric Turbulence in Severe Storms and Cumulus Clouds. NASA TN D-2469, 1964.
11. Crooks, Walter M.; Hoblit, Frederic M.; Mitchel, Finis A.; et. al.: Project HICAT — High Altitude Turbulence Measurements and Meteorological Correlations. AFFDL-TR-68-127, Air Force Flight Dynamics Lab., Nov. 1968.
12. Hoblit, Frederick M.; Paul, Neil; Shelton, Jerry D.; and Ashford, Frances E.: Development of a Power-Spectral Gust Design Procedure for Civil Aircraft. FAA-ADS-53, Federal Aviation Admin., 1966.

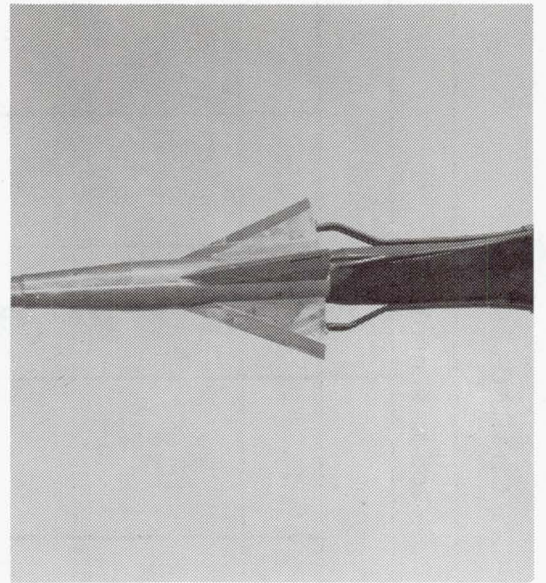
13. Military Specification: Flying Qualities of Piloted Airplanes.
MIL-F-8785B(ASG), 7 Aug. 1969.

TABLE 1.—GUST MEASURING SYSTEM INSTRUMENT CHARACTERISTICS

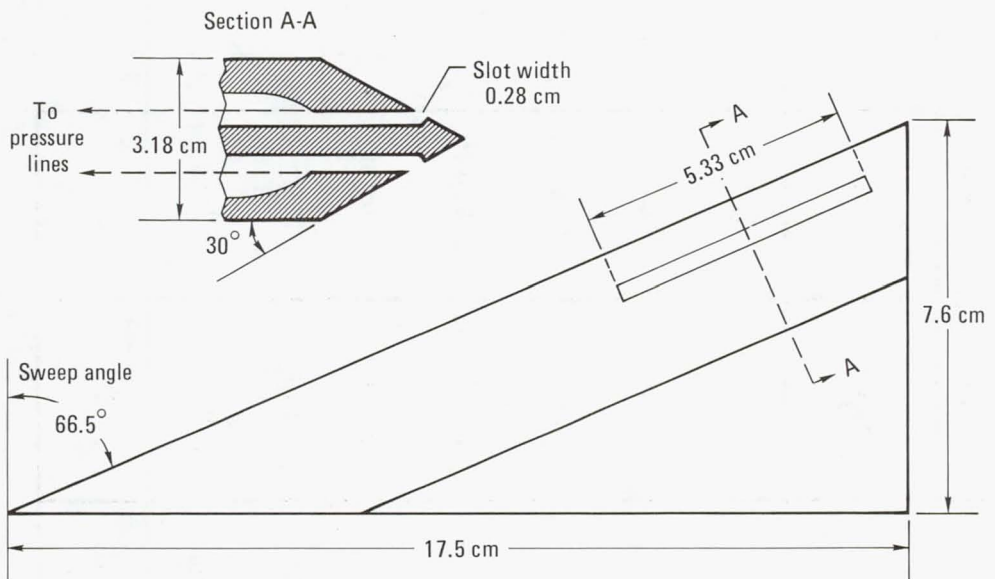
	Pressure measurements		Motion sensors					
	Gust vanes	Dog-leg	Angular rate gyros			Linear accelerometers		
			p	q	r	a_x	a_y	a_n
Natural frequency, Hz	>100	>2000	40	40	40	118	118	118
Presample filter 3 dB break, Hz	40	40	40	40	40	40	40	40
Filter slope, dB/octave	18	18	6	18	18	6	6	6
Encoded range	±13,800 Pa	±20,700 Pa	±20 deg/sec	±20 deg/sec	±20 deg/sec	±1g	±1g	-1, +3g
Encoding increment	3.4 Pa	5.0 Pa	0.08 deg/sec	0.005 deg/sec	0.005 deg/sec	0.004g	0.004g	0.008g
Line length, m	1.3	1.0						
Inside diameter, cm	0.8	0.4						
Natural frequency, Hz (pneumatic)	>55	>70						



(a) Forward quarter view .



(b) Side view .



(c) Vane planform and cross section .

Figure 1.—Gust flow direction vanes .

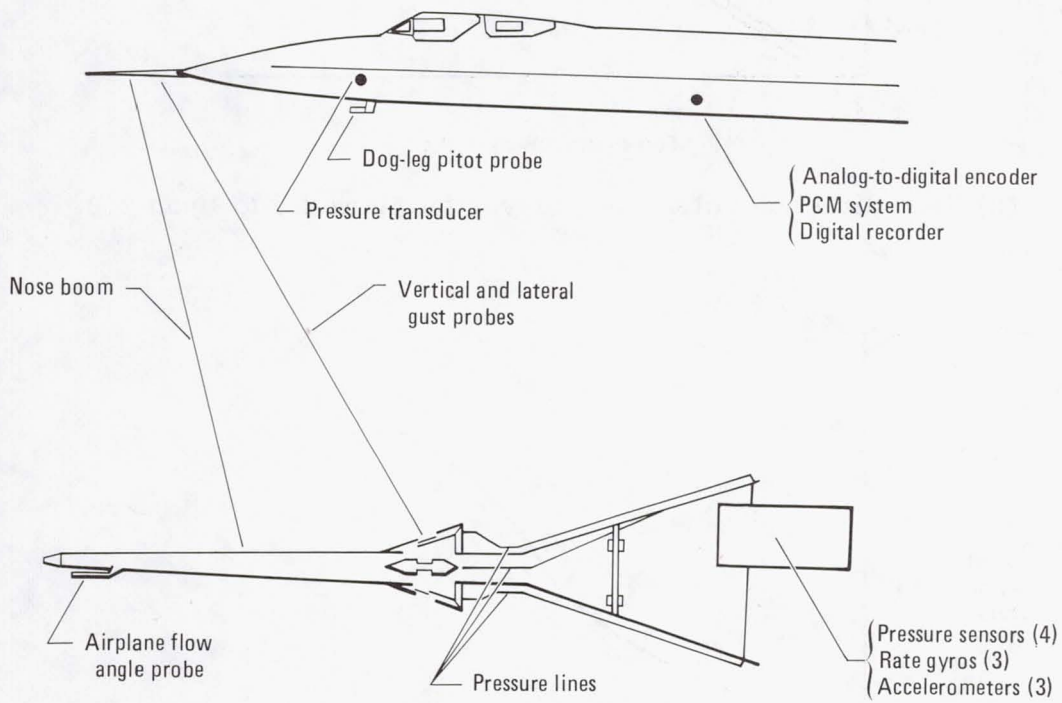
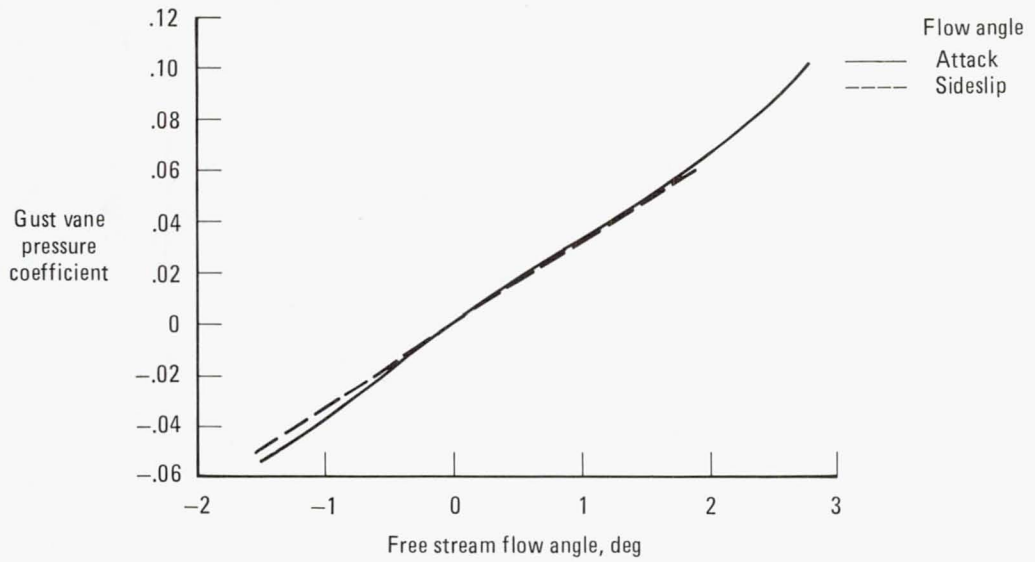
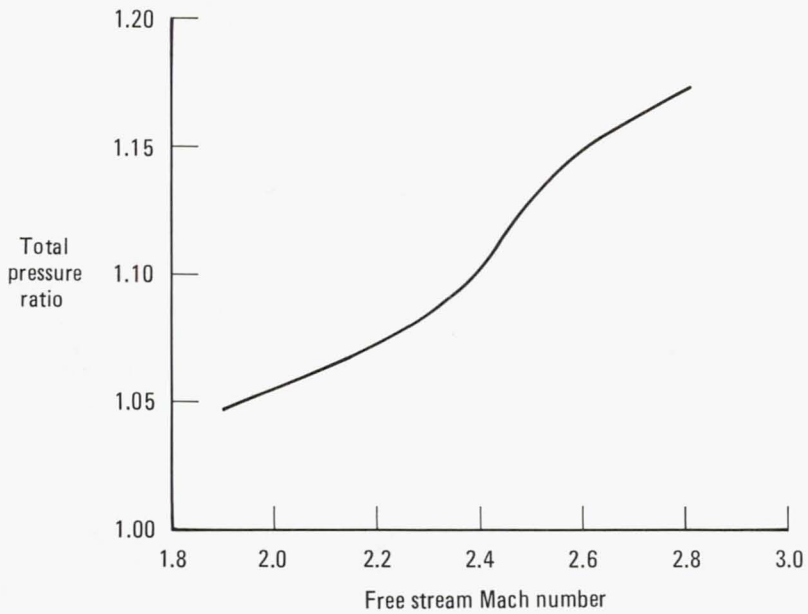


Figure 2.—Locations of gust measurement instrumentation.



(a) Flow direction polynomial curves for Mach 2.2 to Mach 2.8.



(b) Dog-leg Mach number polynomial curve, $C_{P_\alpha} = 0$.

Figure 3.—Gust probe calibration curves.

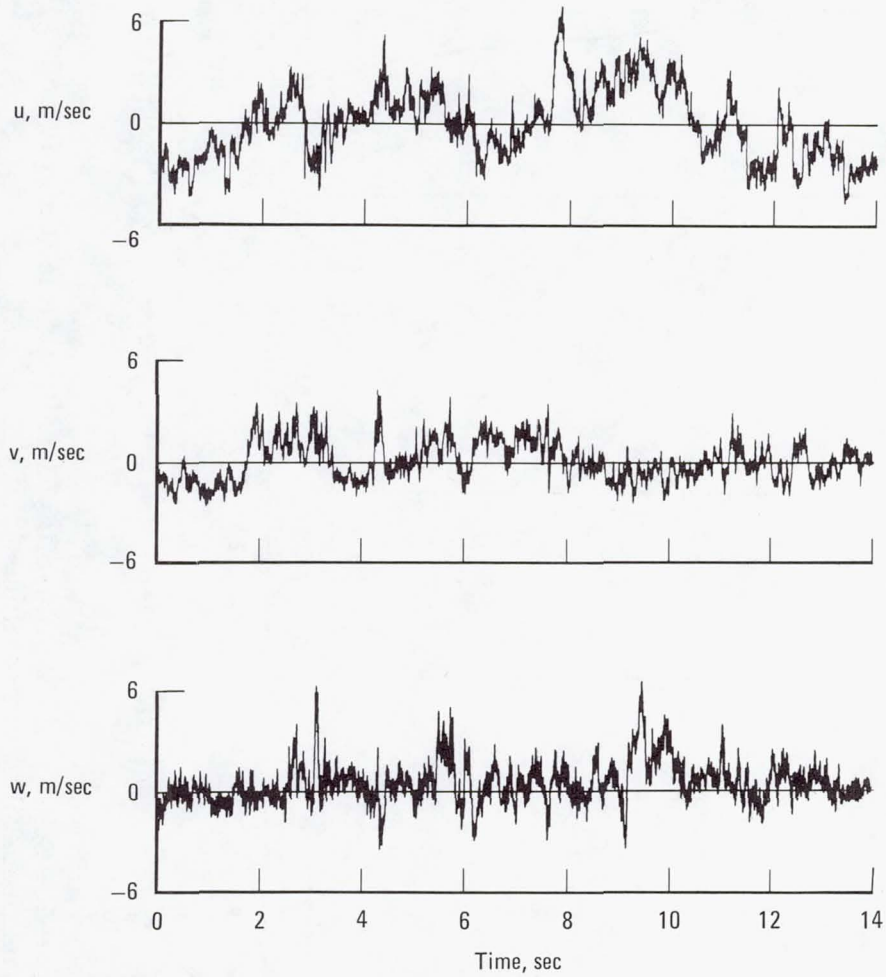
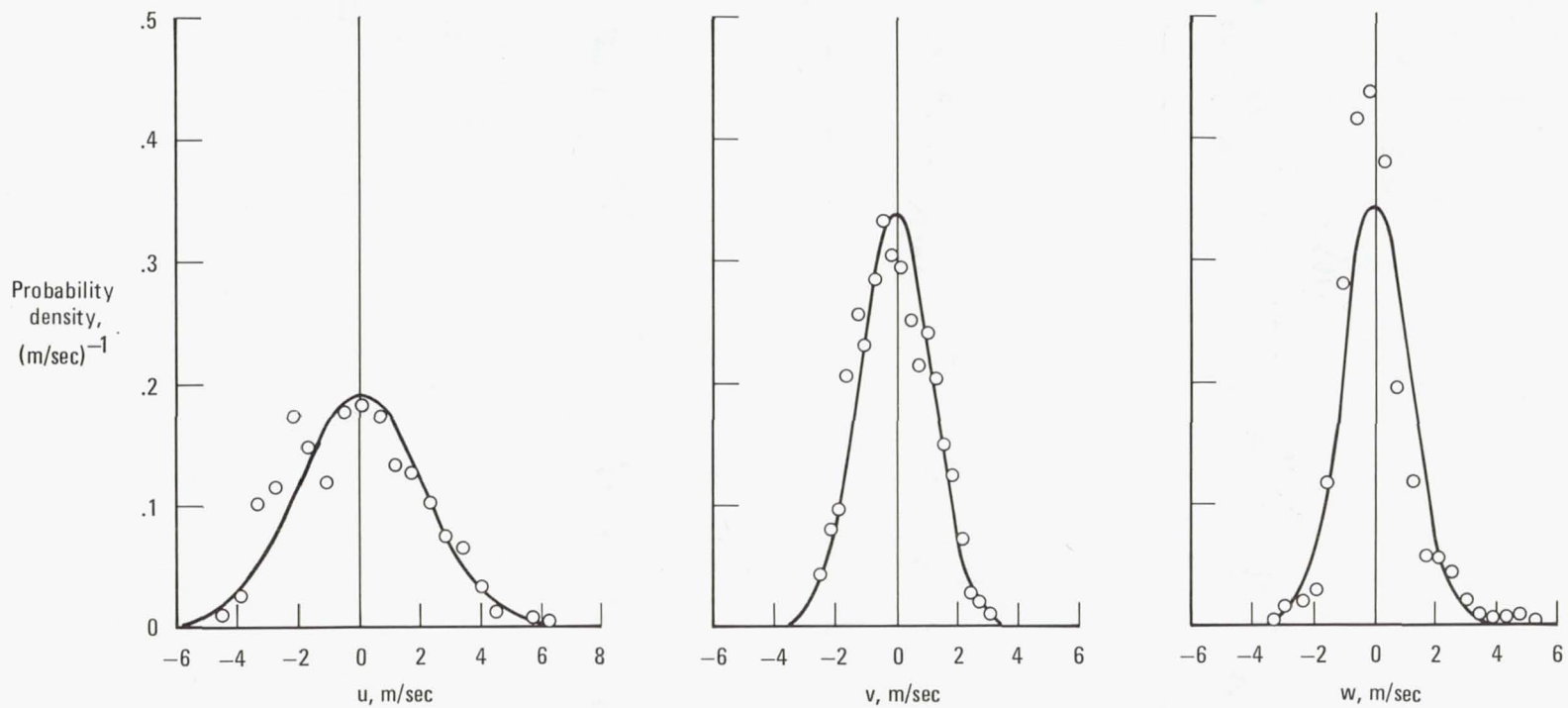


Figure 4.—YF-12 longitudinal, u ; lateral, v ; and vertical, w ; gust velocity time histories measured at 19.8 km altitude.



(a) Longitudinal, rms = 2.15 m/sec. (b) Lateral, rms = 1.17 m/sec. (c) Vertical, rms = 1.15 m/sec.

Figure 5.—Gust velocity probability density (circles) and fitted normal probability curves (lines).

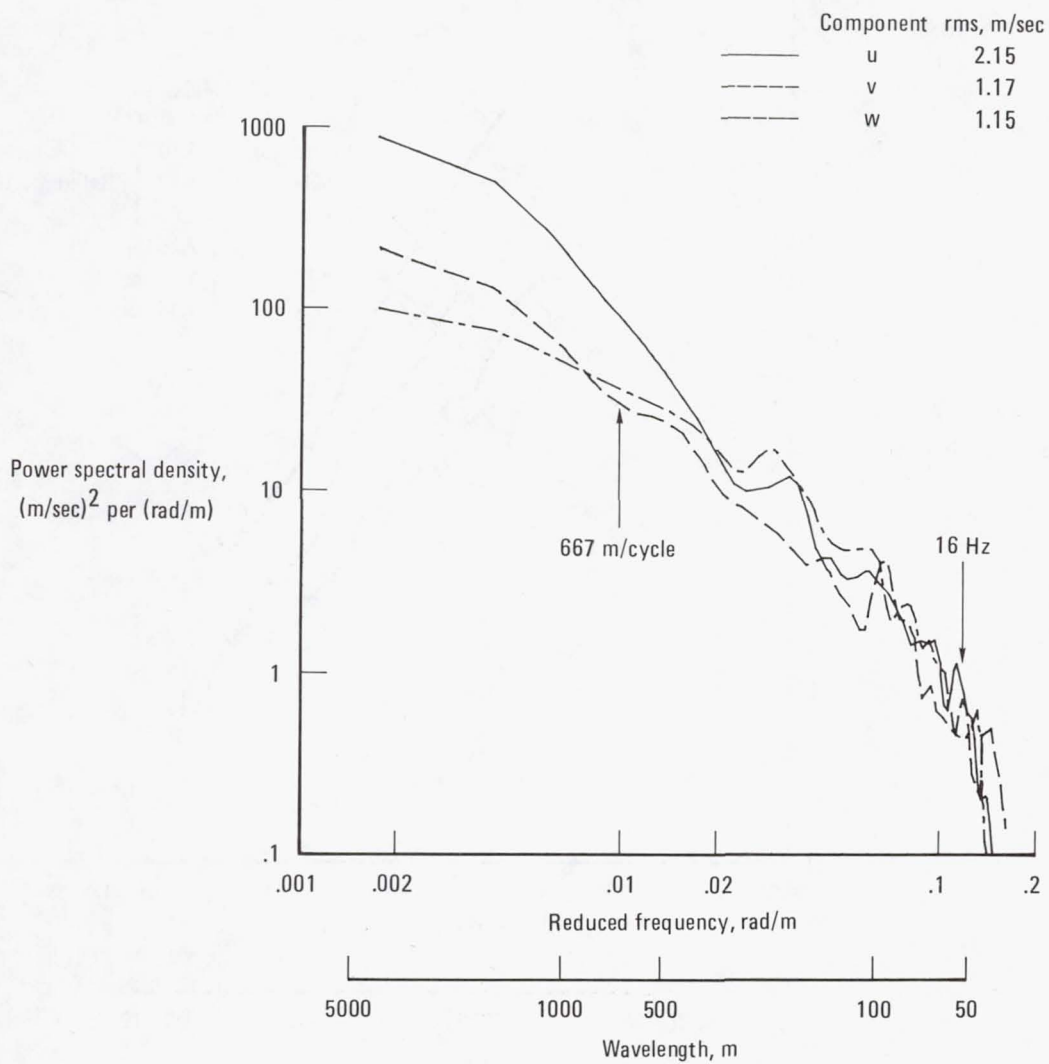


Figure 6.—Gust velocity spectral density (14-second record length, 200 samples per second, 8 degrees of freedom, 7-point Hann-Tukey window).

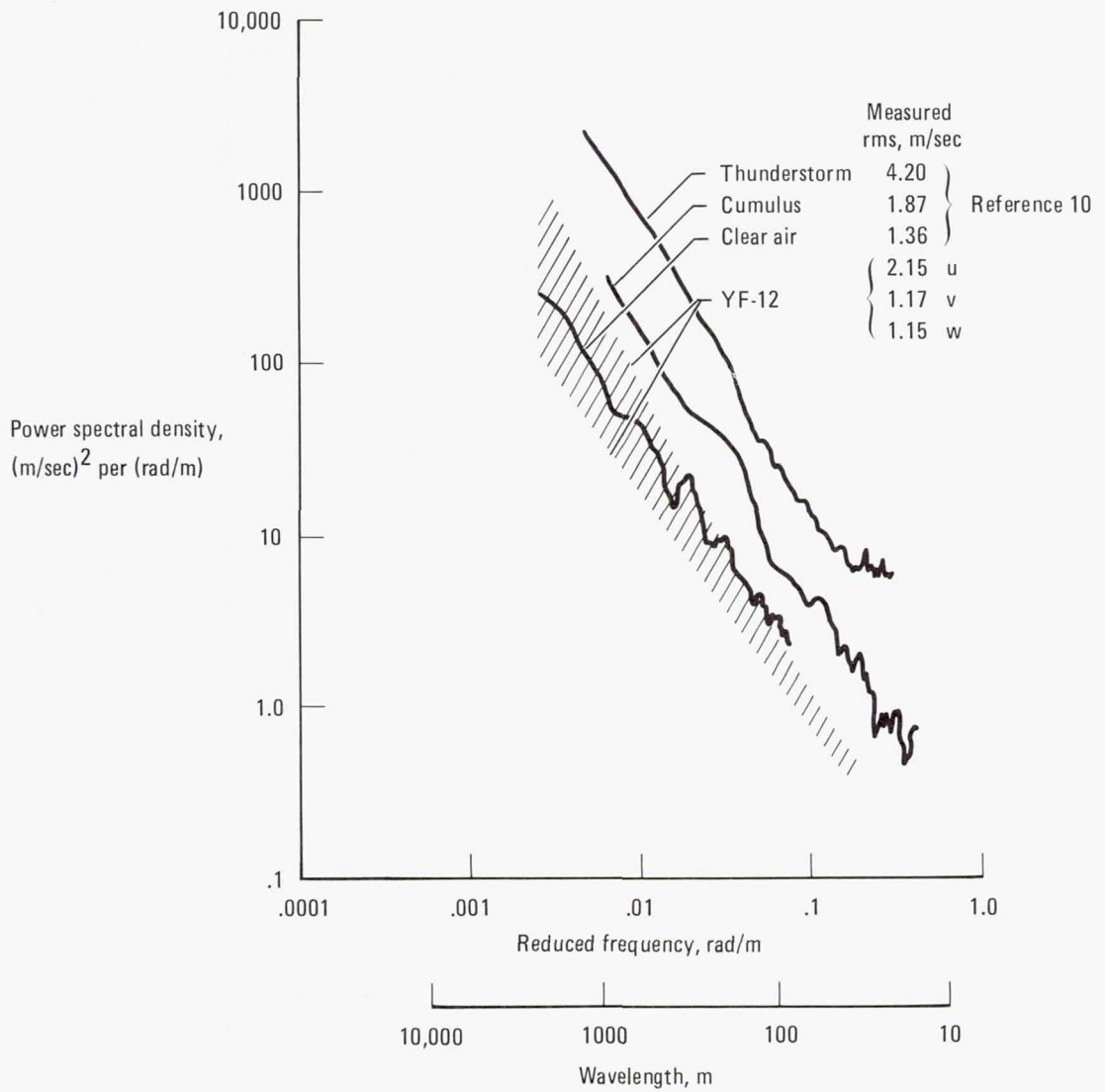


Figure 7.—Spectral densities obtained from lower altitude turbulence phenomena and from the YF-12 at high altitude.